Uluslararası İleri Doğa Bilimleri ve Mühendislik Araştırmaları Dergisi
Sayı 8, S. 49-56, 11, 2024

Araştırma Makalesi

IJANSER
https://as-proceeding.com/index.php/ijanser
ISSN:2980-0811

International Journal of Advanced Natural Sciences and Engineering Researches
Volume 8, pp. 49-56, 11, 2024

Research Article

Assessment of Microstructure of Nanocomposites through Scanning Electron Microscopy, X-ray Diffraction, Thermogravimetric Analysis, and Fourier transform infrared spectroscopy

Shahir Ahmad Safi[*1], Reshteen Ahmad Hemat[1], Mujib Ul Rahman Rahmani[1] and Ali Raza[1]

[1] *Department of Civil Engineering, University of Engineering and Technology Taxila, 47050, Pakistan*

[*]*(safi.researcher@gmail.com)*

(Received: 29 November 2024, Accepted: 05 December 2024)

(3rd International Conference on Recent Academic Studies ICRAS 2024, December 03-04, 2024)

ATIF/REFERENCE: Safi, S. A., Hemat, R. A., Rahmani, M. U. R. & Raza, A. (2024). Assessment of Microstructure of Nanocomposites through Scanning Electron Microscopy, X-ray Diffraction, Thermogravimetric Analysis, and Fourier transform infrared spectroscopy. *International Journal of Advanced Natural Sciences and Engineering Researches*, 8(11), 49-56.

Abstract – The geopolymer composite (GC) mortars have emerged as a promising alternative to traditional cement in promoting sustainable and eco-friendly construction practices. To facilitate the practical use of fiber-reinforced (FR) GC mortars, enhancing their microstructural properties through the incorporation of micro-fibers and nano-particles is critical. This research focuses on improving the microstructural characteristics of fly ash-based GC mortars reinforced with micro basalt fibers (BF) by incorporating varying amounts of nano-Titania. GC mortars were prepared using four Titania dosages (ranging from 1% to 4%) along with 2 wt.% of BF. Additionally, a control mix containing 2% BF but no Titania was produced for comparison. To assess the GC formulations' performance and microstructural characteristics, Fourier Transform Infrared Spectroscopy (FTIR), Thermogravimetric Analysis (TGA), Scanning Electron Microscopy (SEM), and X-ray Diffraction (XRD) were used.

Keywords – Geopolymer Mortar; Nano-Titania; Durability Performance; X-Ray Diffraction (XRD); Structural Analysis; Mechanical Properties; Sustainability.

I. INTRODUCTION

The cement industry's substantial carbon footprint poses a challenge to environmental sustainability. Geopolymer composites (GC) are promising alternatives to Portland cement in concrete construction applications due to their outstanding performance [1-5]. GC mortars function as effective binding materials, created by activating aluminosilicate sources like fly ash using alkaline solutions [6-12]. Over time, GC has demonstrated structural properties that are comparable to or even surpass conventional concrete [13-15]. However, to broaden the practical applications of GC mortars in construction, significant enhancements in their performance through advanced techniques are essential. A key limitation is GC's low early Strength and brittle nature, which restricts its application in areas where higher flexural strength (FS) is required [16]. Therefore, developing efficient and innovative approaches to enhance the structural performance of GC mortars is critical. Incorporating nano-particles and micro-fibers offers potential for improving both mechanical and microstructural properties.

A comprehensive review of the literature reveals a gap in studies addressing the combined use of BF and Titania to evaluate the microstructural characteristics of GC mortar. This study investigates the effect of

varying Titania concentrations on the microstructural properties of basalt-fiber-reinforced (FR) GC mortars. The GC mortars in this research were produced by incorporating 2% BF along with Titania at dosages of 0%, 1%, 2%, 3%, and 4% (wt. %). Scanning Electron Microscopy (SEM), X-ray Diffraction (XRD), Thermogravimetric Analysis (TGA), and Fourier Transform Infrared Spectroscopy (FTIR) were used to assess the impact of Titania on different microstructural characteristics of GC.

II. TESTING PROGRAM

i. Materials

Nano-Titania (P25, 75% anatase, 25% rutile) with particle sizes of 1–30 nm and a purity of 99.68% is used in this study to fabricate GC mortars. The Titania has a specific gravity of 0.24 g/cm³, a median particle size of 20 nm, an anatase-to-rutile ratio of 80:20, and a spherical shape with an LOI below 0.01. Basalt fibers (BF) with a tensile strength of 1800 MPa, an elastic modulus of 70 GPa, and dimensions of 2 mm length and 7 μm diameter reinforce the mortars. Class F fly ash serves as the aluminosilicate precursor, with its chemical properties outlined in Table 2. A binary activator comprising 98% pure NaOH flakes and a sodium silicate solution (30% SiO2, 12.5% Na2O, and 57.4% H2O) is utilized.

Five GC mixes with Titania dosages of 1%, 2%, 3%, and 4% by fly ash mass are prepared and tested for CS, FS, EM, FT, TM, and HN. The alkaline solution-to-fly ash ratio is set at 0.45, while the sodium silicate-to-NaOH ratio is maintained at 2.5 for all mixes [17]. NaOH is dissolved in water and combined with sodium silicate 24 hours before mortar fabrication to create a 12 M alkaline solution. All GC mortars are reinforced with 2% BF. Table 3 details the mortar designs, and Figure 1 provides SEM images of fly ash and nano-Titania particles.

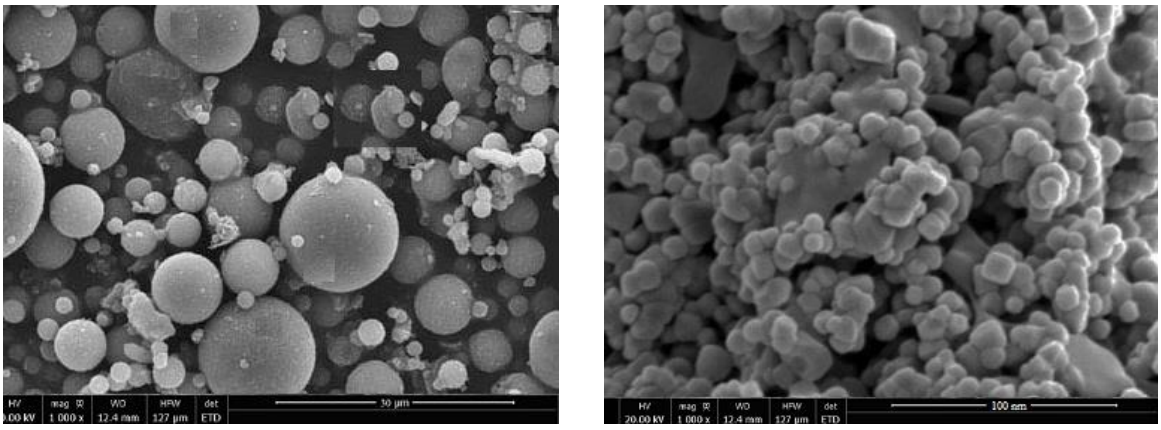

(a) (b)

Figure 1. SEM images of (a) fly ash (b) nano-Titania

Table 3. Mortar design of all five mortars

GC Mortar	BGC-0%NTO	BGC-1%NTO	BGC-2%NTO	BGC-3%NTO	BGC-4%NTO
NaOH (kg)	0.23	0.23	0.23	0.23	0.23
Fly ash (kg)	1.8	1.8	1.8	1.8	1.8
Sodium silicate (kg)	0.58	0.58	0.58	0.58	0.58
Titania (kg)	0	0.01	0.02	0.03	0.04

ii. Development and Testing of Specimens

The GC mortars were prepared using a Hobart mixer. Fly ash and BF were dry blended for five minutes at a low speed during the mixing procedure. Following the completion of the dry mixing of these components, the alkali solution containing different concentrations of Titania was added and rapidly mixed. Until a consistent GC mortar was obtained, this procedure was carried out again. After that, the freshly

made mortars were put into moulds and let to cure for 24 hours at 80°C. To improve their mechanical qualities, the samples were demolded after curing and let to cure for 28 days in the open air.

A field emission SEM was used to examine the surface appearance and failure characteristics of the damaged specimens. This SEM has a magnification range of 1x to 1,000,000x with a resolution of 200 nm at 30 kV. To stop electron charging, the specimens were placed on aluminium stubs, vacuum-dried for 48 hours, and then coated with gold. Under a microscope, the fracture surface morphology and crack propagation were analysed, and failure patterns were recorded.

For XRD analysis, fragments from the damaged specimens obtained from the CS tests were collected and finely ground to achieve particles with less than 2% residue retained on an 80 μm sieve. The XRD analysis was performed using a JEOL JDX-3532 diffractometer with a Cu Kα radiation source (λ = 1.54 Å), operating at 20–40 kV and 2.5–30 mA, scanning a 2θ range of 10–80°. Additionally, a Nicolet 5700 FTIR spectrometer from Thermo Electron Corporation was utilized to analyze absorption spectra in the range of 500–4000 cm^{-1}. Thermogravimetric analysis (TGA) was carried out using a Mettler Toledo TGA/DSC 1 Stare system.

III. RESULTS

i. Microstructural Analysis

The fracture behavior of the GC matrix can be evaluated through SEM analysis by examining its fractured surface. Figure 14 illustrates the SEM analysis for all GC mixtures. The fractured surface of the control sample, which lacks nano-Titania, exhibits notable differences compared to those incorporating nano-Titania. In the control GC mix and the mix with lower amounts of nano-Titania, a significant presence of unreacted or partially reacted fly ash particles along with voids is evident. Conversely, GC mixes containing 2% and 3% nano-Titania display a more compact microstructure. The C-S-H gel formed within the matrix extends among the fly ash particles, functioning as nucleation sites within the pore spaces. This contributes to a denser GC matrix and enhances the bonding efficiency between the Titania nanoparticles. With an increase in the nano-Titania content, the quantity of unreacted fly ash particles decreases, resulting in a more compact matrix and fewer pullout regions for unreacted fly ash. This densification is likely due to the formation of C-S-H gel or C-A-S-H gel facilitated by the interaction between nano-Titania and the fly ash microparticles.

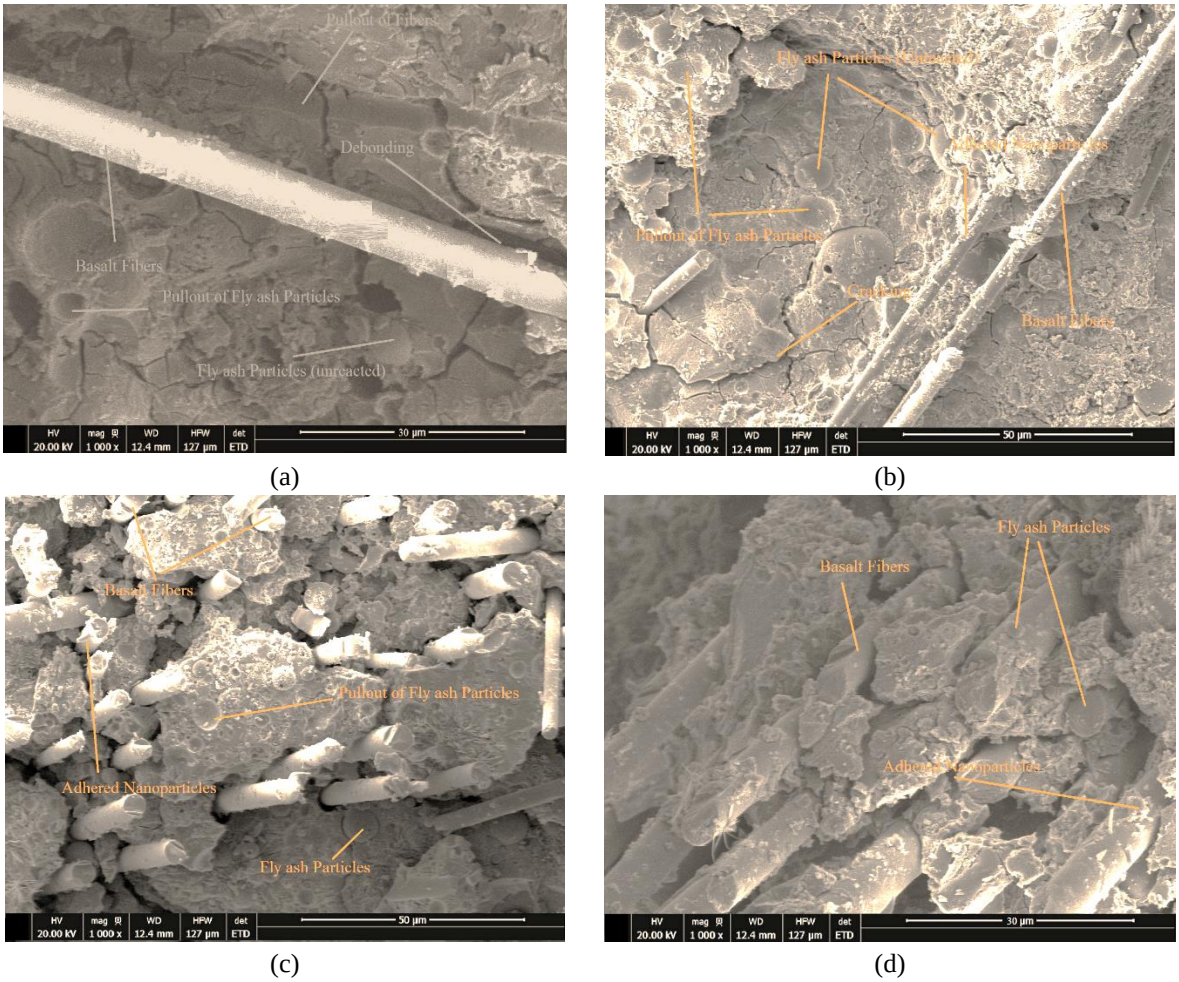

(a) (b)

(c) (d)

Figure 2. SEM images of: (a) BGC-0%NTO (b) BGC-1%NTO (c) BGC-2%NTO (d) BGC-3%NTO

The nanoparticles of Titania functioned as load carriers, facilitating the transfer process and halting the progression of micro-cracks. Increasing the amount of nano-Titania reduced the appearance of cracks, resulting in a more compact GC matrix. At this point, nano-Titania contributed to minimizing micro-crack formation by creating bonds with the by-products generated during GC hydration reactions. SEM analysis also reveals strong bonding between the BF and the GC matrix, likely due to the ability of nano-Titania to enhance internal adhesion and form a denser microstructure within the GC mix. Observations from SEM images indicate some pullout of unreacted fly ash particles and limited BF. Figure 14 illustrates that the GC's alkaline environment does not negatively impact the BF. A minimal amount of polymerization products adheres to the BF's surface, likely because of its grooved texture, which supports robust bonding within the GC matrix.

ii. XRD Analysis

Figure 12 shows the X-ray diffraction (XRD) patterns for the FA-based GC (which acts as the baseline) and those that include 1%, 2%, and 3% nano calcium carbonate. When an amorphous GC binder forms, the significant diffuse peak seen in the raw FA diffractograms within the 2θ range of 15° to 35° moves to 18° to 40° (Figure 12), increasing mechanical strength [18]. It is clear that some of the mineral phases found in FA, including mullite, magnetite, haematite, and quartz, can still be found in FA-based GC both with and without the nano calcium carbonate component. This suggests that these minerals enhanced the GC matrix by acting as micro-aggregates or fillers and did not take part in the geopolymerization activity [19]. Moreover, between 18° and 40° (2θ), the hump's intensity increases, possibly as a result of the breakdown

of nano calcium carbonate particles. This dissolution may help the GC network grow by forming calcium silicate hydrate (CSH) in addition to sodium aluminosilicate (NASH), the major binder. These results are consistent with earlier study published in the literature, in which scientists mixed different calcium-based substances with other aluminosilicates (such as slag, FA, and metakaolin) during GC synthesis [20-22]. These studies have consistently demonstrated that incorporating calcium compounds enhances the mechanical performance of the resulting materials.

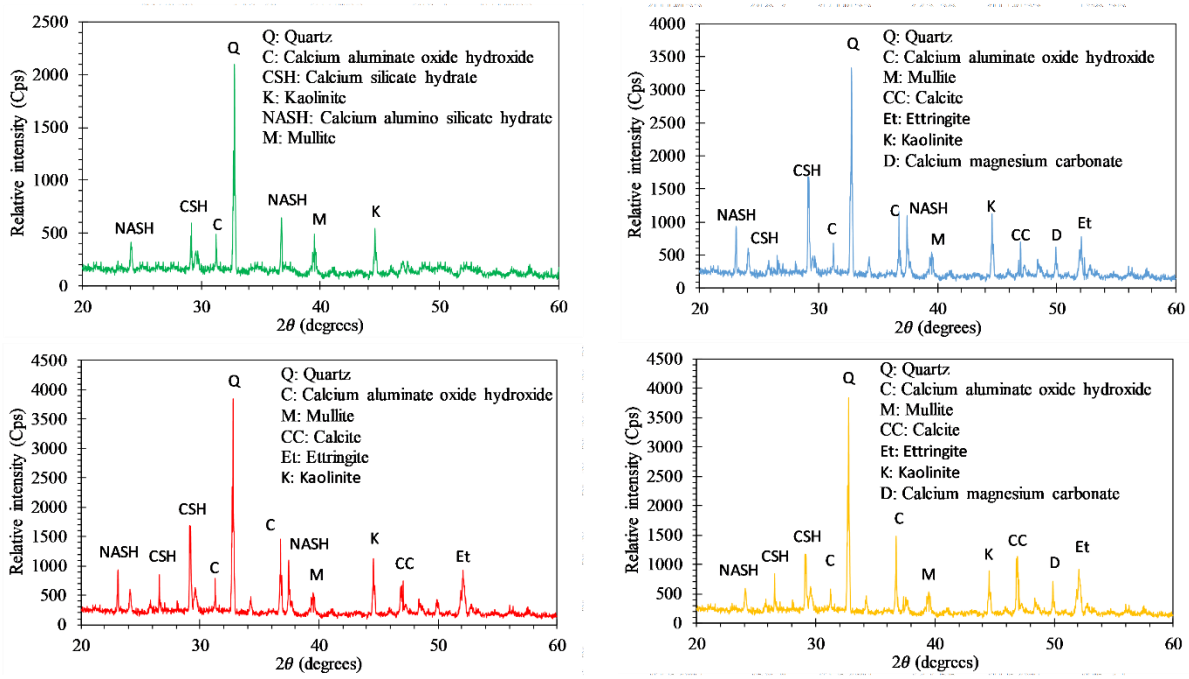

Figure 3. XRD diffraction patterns of (a) BGC-0%NTO (b) BGC-1%NTO (c) BGC-2%NTO (d) BGC-3%NTO

iii. FTIR Spectroscopy

The FA-based GC used as a reference and the GCs with 1, 2, and 3% of the additive (nano calcium carbonate; n-CC) are shown in Figure 13. It is evident that the O-H bond vibrations in water molecules is linked to the broad bands in the GC spectra located at 3352, 3354, 3363, and 3358 cm−1. In samples containing the additive (1.0, 2.0, and 3.0% of n-CC), these bands are more noticeable and intense. This could be a sign of a larger water content in the GC network, which could affect the strength in mechanical testing. The bending vibrations of H-O-H from interlayer adsorbed water molecules are responsible for the weak absorption bands about 1645 cm−1 [23]. The stretching of carbonate groups CO32− is represented by the bands around 1340–1381 cm−1 [24]. When nano calcium carbonate is added, this band gets stronger, which may indicate that divalent calcium cations (Ca2+) were added to the GC structure as network formers. This finding is consistent with the work of Djobo et al. [25], who created GC binder by combining oyster shells with volcanic ash. Their results showed that greater energy absorption bands are produced when calcium is combined with carbonate groups as opposed to when Na-carbonate is used. The asymmetric stretching of Si-O-Al bonds, a distinctive peak of GC binder, is linked to the absorption bands in the 949–961 cm−1 region [26, 27]. Lastly, the bands at about 796 cm−1 represent the Si-O bond vibration modes in quartz mineral [28].

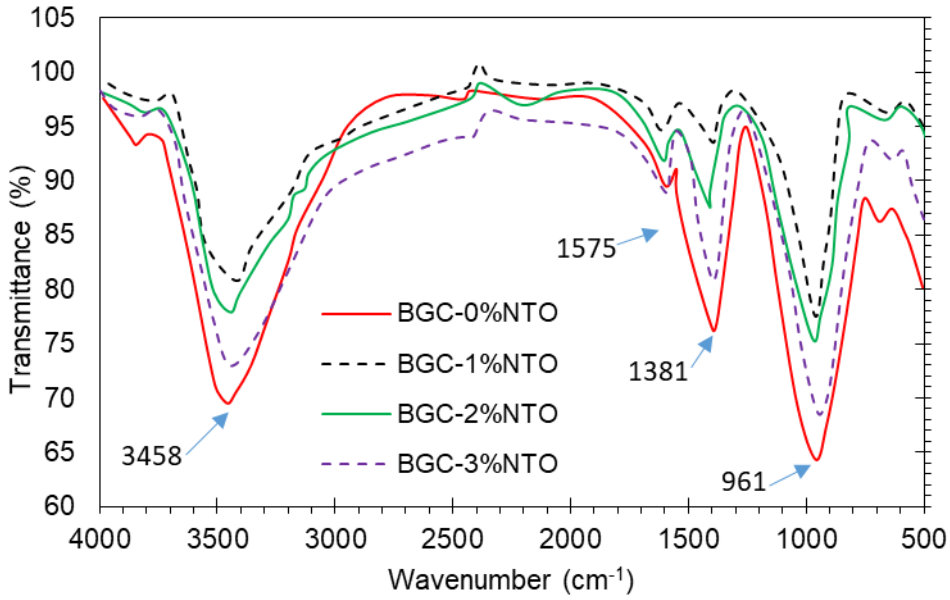

Figure 4. FTIR spectra of (a) BGC-0%NTO (b) BGC-1%NTO (c) BGC-2%NTO (d) BGC-3%NTO

iv. Thermogravimetric Analysis

The thermogravimetric analysis (TGA) of FA-based GC with 0%, 1%, 2%, and 3% nano calcium carbonate particles is shown in Figure 14. Up to 200 °C, a consistent weight loss was seen in all thermograms; however, between 200 and 800 °C, the rate of weight loss sharply decreased. For the FA-based GC with 0%, 1%, 2%, and 3% additive, the corresponding weight reductions were 1%, 2%, 4%, and 5%, respectively. The release of water that is chemically bonded to the GC matrix is the cause of these losses [29]. The higher the calcium carbonate level, the greater the loss. FTIR study, which showed a greater concentration of FA-nano particle mixes, is in line with this result. By adding n-CC to the GC formulation, calcium silicate hydrate (CSH) and the primary binder, amorphous Na-aluminosilicate (NASH), may form. Consequently, the removal of structural water from these binder phases is responsible for the notable weight reduction in the TG curves.

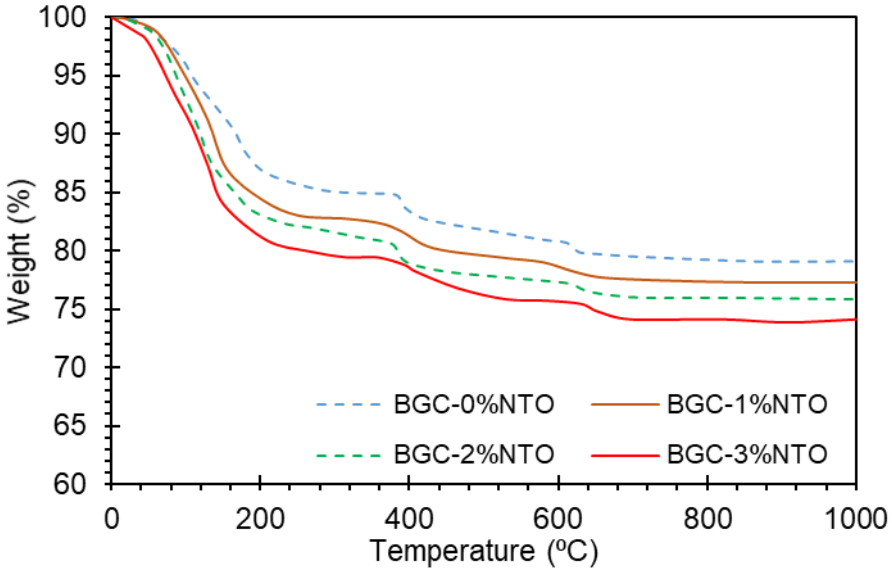

Figure 5. TGA of (a) BGC-0%NTO (b) BGC-1%NTO (c) BGC-2%NTO (d) BGC-3%NTO

IV. CONCLUSION

The current experimental investigation aimed to assess the mechanical and fracture characteristics of micro-basalt FR-GC mortar incorporating varying proportions of nano-Titania. The following key findings were derived from this study:

1. SEM images indicated that the inclusion of nano-Titania contributes to a more compact structure by filling the nano-voids between fly ash micro-particles in the GC matrix. The images also revealed that the interaction between the BF and GC structure shows efficient interlocking, which could be attributed to the capability of nano-Titania to refine and densify the GC matrix.
2. The hump's intensity increased between 18° and 40°, according to XRD analysis. This is probably because the n-CC nanoparticles dissolved, forming calcium silicate hydrate (CSH) in combination with the primary binder, such as sodium aluminosilicate (NASH), which enlarged the GC network. The O-H bond vibrations in water molecules is linked to the large peaks in the GC spectra that are seen at 3352, 3354, 3363, and 3369 cm−1. In specimens including the additive, these peaks are bigger and more noticeable, which might be because the GC network has more water, which could affect the strength.

REFERENCES

[1] Wang, J., et al., Study on the optimum initial curing condition for fly ash and GGBS based geopolymer recycled aggregate concrete. Construction and Building Materials, 2020. 247: p. 118540.
[2] Ali, N., et al., Evaluation of the 12–24 mm basalt fibers and boron waste on reinforced metakaolin-based geopolymer. Construction and Building Materials, 2020. 251: p. 118976.
[3] Mehta, A. and R. Siddique, Properties of low-calcium fly ash based geopolymer concrete incorporating OPC as partial replacement of fly ash. Construction and Building Materials, 2017. 150: p. 792-807.
[4] Patel, Y.J. and N. Shah, Development of self-compacting geopolymer concrete as a sustainable construction material. Sustainable Environment Research, 2018. 28(6): p. 412-421.
[5] Ranjbar, N. and M. Zhang, Fiber-reinforced geopolymer composites: A review. Cement and Concrete Composites, 2020. 107: p. 103498.
[6] Provis, J.L. and S.A. Bernal, Geopolymers and related alkali-activated materials. Annual Review of Materials Research, 2014. 44: p. 299-327.
[7] Alhazmi, H., et al., Utilization of Polymer Concrete Composites for a Circular Economy: A Comparative Review for Assessment of Recycling and Waste Utilization. Polymers, 2021. 13(13): p. 2135.
[8] Mahmood, A., et al., Geopolymers and Fiber-Reinforced Concrete Composites in Civil Engineering. Polymers, 2021. 13(13): p. 2099.
[9] Napoli, A. and R. Realfonzo, RC columns strengthened with novel CFRP systems: An experimental study. Polymers, 2015. 7(10): p. 2044-2060.
[10] Quiatchon, P.R.J., et al., Investigation on the compressive strength and time of setting of low-calcium fly ash geopolymer paste using response surface methodology. Polymers, 2021. 13(20): p. 3461.
[11] Rashedi, A., et al., Mechanical, fracture, and microstructural assessment of carbon-fiber-reinforced geopolymer composites containing Na2O. Polymers, 2021. 13(21): p. 3852.
[12] Raza, A., et al., On the Structural Performance of Recycled Aggregate Concrete Columns with Glass Fiber-Reinforced Composite Bars and Hoops. Polymers, 2021. 13(9): p. 1508.
[13] Adesina, A., Performance and sustainability overview of alkali-activated self-compacting concrete. Waste Disposal & Sustainable Energy, 2020: p. 1-11.
[14] Duxson, P., et al., Geopolymer technology: the current state of the art. Journal of materials science, 2007. 42(9): p. 2917-2933.
[15] Zhuang, X.Y., et al., Fly ash-based geopolymer: clean production, properties and applications. Journal of Cleaner Production, 2016. 125: p. 253-267.
[16] Alomayri, T., A. Raza, and F. Shaikh, Effect of nano SiO2 on mechanical properties of micro-steel fibers reinforced geopolymer composites. Ceramics International, 2021.
[17] Alomayri, T., Performance evaluation of basalt fiber-reinforced geopolymer composites with various contents of nano CaCO3. Ceramics International, 2021.
[18] Bayiha, B.N., et al., Effect of limestone dosages on some properties of geopolymer from thermally activated halloysite. Construction and Building Materials, 2019. 217: p. 28-35.
[19] Tchakoute, H., et al., Influence of gibbsite and quartz in kaolin on the properties of metakaolin-based geopolymer cements. Applied Clay Science, 2015. 107: p. 188-194.
[20] Yusuf, M.O., et al., Strength and microstructure of alkali-activated binary blended binder containing palm oil fuel ash and ground blast-furnace slag. Construction and Building Materials, 2014. 52: p. 504-510.

[21] Yip, C.K., G. Lukey, and J.S. Van Deventer, The coexistence of geopolymeric gel and calcium silicate hydrate at the early stage of alkaline activation. Cement and concrete research, 2005. 35(9): p. 1688-1697.
[22] Yip, C.K., et al., Effect of calcium silicate sources on geopolymerisation. Cement and Concrete Research, 2008. 38(4): p. 554-564.
[23] Shaikh, F., Y. Shafaei, and P. Sarker, Effect of nano and micro-silica on bond behaviour of steel and polypropylene fibres in high volume fly ash mortar. Construction and Building Materials, 2016. 115: p. 690-698.
[24] Hosan, A. and F.U.A. Shaikh, RETRACTED: influence of nano-CaCO3 addition on the compressive strength and microstructure of high volume slag and high volume slag-fly ash blended pastes. 2020, Elsevier.
[25] Djobo, J.Y., et al., Synthesis of geopolymer composites from a mixture of volcanic scoria and metakaolin. Journal of Asian Ceramic Societies, 2014. 2(4): p. 387-398.
[26] Alomayri, T., F. Shaikh, and I.M. Low, Mechanical and thermal properties of ambient cured cotton fabric-reinforced fly ash-based geopolymer composites. Ceramics International, 2014. 40(9): p. 14019-14028.
[27] Nana, A., et al., Room-temperature alkaline activation of feldspathic solid solutions: development of high strength geopolymers. Construction and Building Materials, 2019. 195: p. 258-268.
[28] Nobouassia Bewa, C., et al., Water resistance and thermal behavior of metakaolin-phosphate-based geopolymer cements. Journal of Asian Ceramic Societies, 2018. 6(3): p. 271-283.
[29] Shaikh, F.U. and S.W. Supit, Mechanical and durability properties of high volume fly ash (HVFA) concrete containing calcium carbonate (CaCO3) nanoparticles. Construction and building materials, 2014. 70: p. 309-321.